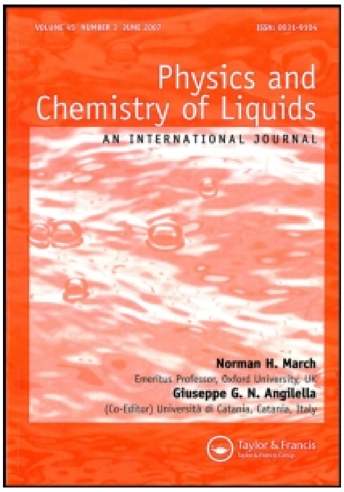

Physics and Chemistry of Liquids

Publication details, including instructions for authors and subscription information:
http://www.informaworld.com/smpp/title~content=t713646857

Thermodynamic and Structural Interpretations of the Undercooled Liquid Metals

R. N. Singh[a b]; F. Sommer[a]
[a] Max-Planck-Institut für Metallforschung, Institut für Werkstoffwissenschaft, Stuttgart, Germany [b] Department of Physics, Sultan Qaboos University, Al-Khod, Sultanate of Oman

To cite this Article Singh, R. N. and Sommer, F.(1994) 'Thermodynamic and Structural Interpretations of the Undercooled Liquid Metals', Physics and Chemistry of Liquids, 28: 2, 129 — 140

To link to this Article: DOI: 10.1080/00319109408029548

URL: http://dx.doi.org/10.1080/00319109408029548

Phys. Chem. Liq., 1994, Vol. 28, pp. 129–140
Reprints available directly from the publisher
Photocopying permitted by license only

THERMODYNAMIC AND STRUCTURAL INTERPRETATIONS OF THE UNDERCOOLED LIQUID METALS

R. N. SINGH* and F. SOMMER

Max-Planck-Institut für Metallforschung, Institut für Werkstoffwissenschaft, Seestr. 75, D-70174 Stuttgart, Germany

(Received 7 July 1993)

A simple scheme based on pseudopotential and hard sphere results is used to evaluate the specific heat in the undercooled region ($T < T_m$) and in the higher temperature region ($T > T_m$) of liquid metals Na, K, Rb and Cs. The structure dependent part of the specific heat is found to increase in the undercooled region ($T < T_m$) with decreasing temperature and exhibits an inflection at a given temperature (T_I). The results are discussed in the light of energetics and direct correlation function. We have also computed the diffusion coefficients which show T^2-dependence in the undercooled region.

KEY WORDS: Specific heat, diffusion coefficient.

1 INTRODUCTION

It is becoming increasingly evident that the temperature dependent thermodynamic functions should better be used to analyse the energetics as well as the configurational details of the liquid metals, particularly, in the undercooled ($T \ll T_m$, T_m is the melting temperature) and also in the very high ($T \gg T_m$) temperature region. For example, C_p (specific heat at constant pressure) of liquid metals having high melting points ($T_m > 900\,\mathrm{K}$) remains constant [1] over a wide range of temperatures above T_m, whereas C_p increases with decreasing temperature in the undercooled region and in a small temperature range above T_m for several metals with $T_m < 900$ K [2].

Then the obvious points that needed to be addressed are (i) what happens in the undercooled region and in the very high temperature region, (ii) whether these informations could be used to analyse the energetics and the structure of the undercooled metastable state. Due to extreme experimental conditions, a direct measurement of any of the physical quantities of interest is enormously difficult and, therefore, a theoretical analysis is very much useful. Nevertheless, such investigations are of primary importance to understand the physical processes that are linked to metallic glass formation [3–6] or phenomenon of rapid solidification [7–9].

In the present work we make use of a theoretical scheme to address the above mentioned points. It is based on pseudopotential perturbation theory, the thermo-

---

*Present address: Department of Physics, Sultan Quaboos University, P.O. Box 32486, Al-Khod, Sultanate of Oman.

dynamics of hard sphere systems and the variational method based on Gibbs–Bogoliaubov inequality. This has been proved extremely successful to discuss the physical processes associated with s–p bonded liquid metals near the melting point (for recent review see Young [10]). Here we apply it to extract informations in the undercooled region with special emphasis to C_p, the static structure factor $S(q)$ and the diffusion coefficient (D). The necessary theoretical scheme is outlined in section 2, while section 3 contains the results and discussion for C_p. It follows a short discussion on structure factor in section 4. The results for D are provided and discussed in section 5. It follows a short conclusion.

2 THEORY

The heart of the problem is to establish a successful link between the pseudopotential, the structure and the thermodynamic function. The variational method [11] based on Gibbs–Bogoliaubov inequality paves the way, i.e.

$$\left(\frac{\partial F}{\partial \sigma}\right)_{\Omega,T}=0 \tag{1}$$

where F is the Helmholtz free energy at a given temperature T and the volume Ω of the system. σ is the hard sphere diameter. F can be expressed as

$$F=E-TS \tag{2}$$

E is the internal energy and S is the entropy at T. For simple s–p bonded liquid metals, one can safely express,

$$E=E_{\text{elec}}+E_{\text{elec-ion}}+E_{\text{ion}} \tag{3}$$

E_{elec} is the energy of the homogeneous electron gas which is the sum of the kinetic energy of electrons, exchange energy, correlation energy and the low temperature specific heat contribution for the electron gas. By adding them together, one writes

$$E_{\text{elec}}=Nz\left\{\frac{3}{10}K_F^2-\frac{3}{4\pi}K_F-0.0474-0.0155\ln K_F-\frac{1}{2}\left(\frac{\pi K_B}{K_F}\right)^2T^2\right\} \tag{4}$$

K_F is the fermi wave vector ($K_F^3=3\pi^2 z/\Omega$, z is the valency, and Ω is the atomic volume), and K_B is the Boltzmann constant. The contribution, $E_{\text{elec-ion}}$, which arises due to electron-ion interaction has been evaluated in the framework of pseudopotential perturbation theory [12], i.e.

$$E_{\text{elec-ion}}=\lim_{q\to 0}\left(W^0(q)+\frac{4\pi z}{q^2}\right)\frac{z}{\Omega}+\frac{1}{16\pi^3}\int_0^\infty (W^0(q))^2S(q)\left\{\frac{1}{\varepsilon^*(q)}-1\right\}q^4\,dq \tag{5}$$

where q is the wave vector. The first term on right-hand side is the first order energy and second is the band structure energy. $W^0(q)$ is the unscreened form factor and is obtained by taking the Fourier transform of the r-space potential seen by conduction electrons in the presence of ions.

In past a great effort has been made to model the electron-ion potential. Presently we consider the Heine–Abarenkov (HA) [13] form of model potential $W^0(r)$, which consists of a well-depth (A) for the core region $r < r_m$, r_m is the chosen model radius and it is Coulombic ($-z/r$) in nature in the outside region ($r > r_m$). This is preferable because it has rigorous theoretical foundation (see Cohen and Heine [14]) and also the model parameters (A, r_m) occurring here are not fitted to any of the observed properties but are determined independently by matching the wave functions [15]. The Fourier transform of $W_0(r)$ becomes

$$W_0(q) = -\frac{4\pi z}{\Omega q^2}\cos qr_m - \frac{4\pi A}{\Omega q^3}\{\sin qr_m - qr_m \cos qr_m\} \tag{6}$$

$\varepsilon^*(q)$ in Eq. (5) is the modified Hartree dielectric screening function which takes into account of the conduction electrons interaction,

$$\varepsilon^*(q) = 1 + \{\varepsilon(q) - 1\}\{1 - G(q)\} \tag{7}$$

$\varepsilon(q)$ is the Hartree dielectric function and $G(q)$ is the correction term for the exchange and correlated motion of the conduction electrons. We use here the modified Hubbard formula, i.e.

$$G(q) = \frac{q^2}{2(q^2 + \gamma K_F^2)} \tag{8}$$

The function γ has been introduced to satisfy the compressibility sum rule. By making use of the interpolation scheme of Nozier and Pines [16], γ is given [17] by

$$\gamma = \frac{2\pi}{\pi K_F + 0.153} \tag{9}$$

The structure factor, $S(q)$, for liquid metals appearing in Eq. (5) can be calculated [18] from the Percus–Yevick solution for hard sphere fluids which is characterized by the hard sphere diameter (σ) or, equivalently, by the packing fraction $\eta = (\pi/6\Omega)\sigma^3$. $S(q)$ also occurs as the basic input to calculate [11] energy, E_{ion}, i.e.

$$E_{\text{ion}} = \frac{3}{2}K_B T + \frac{z^2}{\pi}\int_0^\infty \{S(q) - 1\}\,dq \tag{10}$$

The same η which is required for the calculation of $S(q)$ can readily be used to evaluate the entropy, S, of the hard sphere fluids, i.e.

$$S = S_{\text{gas}} + S_\eta + S_{\text{elec}} \tag{11}$$

Table 1 Coefficients for *Na, K, Rb* and *Cs*.

Metal	a_0	a_1 $\times 10^{-4}$	a_2 $\times 10^{-7}$	a_3 $\times 10^{-10}$	a_4 $\times 10^{-14}$
Na	0.643	− 6.831	6.327	− 3.286	5.158
K	0.634	− 8.067	9.240	− 6.633	19.481
Rb	0.678	− 12.939	23.433	− 25.478	112.187
Cs	0.674	− 12.653	23.217	− 25.876	116.477

with

$$S_{\text{gas}} = \frac{5}{2}K_B + K_B \ln\left\{\Omega\left(\frac{2\pi m K_B T}{h^2}\right)^{3/2}\right\} \tag{12}$$

$$S_\eta = K_B \eta(3\eta - 4)(1-\eta)^{-2} \tag{13}$$

$$S_{\text{elec}} = zK_B^2 T\left(\frac{\pi\Omega}{3z}\right)^{2/3} \tag{14}$$

Here m is the atomic mass and h is the Plancks constant. The purpose of the present scheme is evident by now. Equation (1) establishes a link between the structure, the potential and the thermodynamic function through the packing fraction η. At each temperature, the optimisation condition (1) has been carried out repeatedly to ensure minimum Helmholtz free energy for the system with respect to σ and hence the packing fraction η. The densities appropriate to pure liquid metals at relevant temperatures have been calculated from Smithels [19] metal book. The values of η computed for Na, K, Rb and Cs are then represented as a power series in terms of temperature T in the form

$$\eta = a_0 + a_1 T + a_2 T^2 + a_3 T^3 + a_4 T^4 \tag{15}$$

where a_0, a_1, a_2, a_3 and a_4 are coefficients and are tabulated in Table 1. A similar $\eta - T$ dependence has also been used [20] successfully to calculate the enthalpy and the compressibility of liquid alkali metals above T_m.

3 SPECIFIC HEAT

Once the T-dependence of η is established, then the specific heat C_p can be calculated, as

$$C_p = T\left(\frac{\partial S}{\partial T}\right)_p \tag{16}$$

In view of Eq. (11), one writes

$$C_p = C_p^{\text{gas}} + C_p^{\eta} + C_p^{\text{elec}} \tag{17}$$

with

$$C_p^{\text{gas}} = K_B\{1.5 + \alpha T\} \tag{18}$$

$$C_p^{\eta} = -2K_B T(2-\eta)(1-\eta)^{-3}\left(\frac{\partial \eta}{\partial T}\right)_p \tag{19}$$

$$C_p^{el} = K_B S_{\text{el}}\left(1 + \frac{2}{3}T\alpha\right) \tag{20}$$

Here α is the thermal coefficient of expansion. The values of C_p for Na, K, Rb and Cs computed for both high ($T > T_m$) and undercooled region ($T < T_m$) are displayed in Figure 1. Above T_m, C_p of Na, K, Rb, Cs decreases with increasing temperature. In the undercooled ($T < T_m$) region, however, C_p increases with decreasing temperature till it reaches a point of inflection in C_p. Other theoretical investigations [21] also suggest a anomaly in C_p at a particular temperature in Ga, Tl and Ti.

The increasing tendency of C_p in the undercooled region has, in particular, been noticed experimentally for several low melting metals (e.g. indium, tin and bismuth [22]).

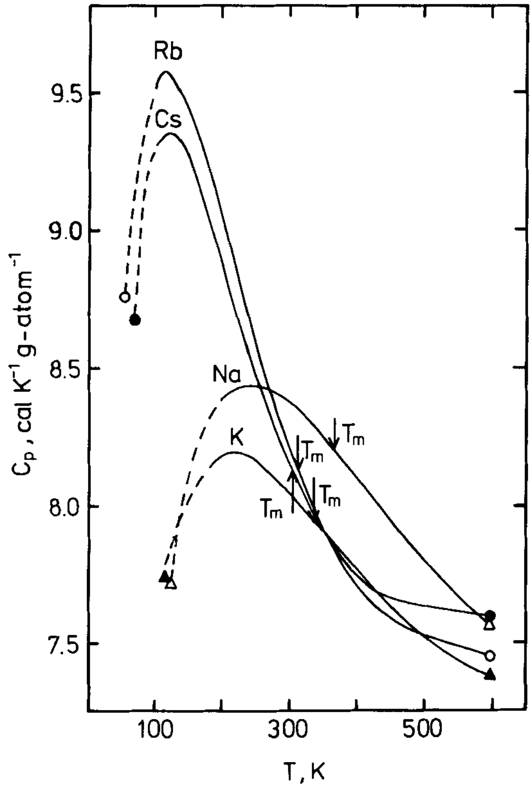

Figure 1 Specific heat at constant pressure. C_p (cal K^{-1} g-atom^{-1}) in the undercooled ($T < T_m$) and in the high temperature range ($T > T_m$) for liquid alkali metals: Na(△△), K(▲▲), Rb (○○) and Cs (●●).

The gradient of C_p in the undercooled region and the temperature (T_I) at which C_p undergoes inflection seem to be related to the melting temperature (T_m) of the metal. For example, Rb and Cs having lower T_m exhibit larger gradient in C_p than Na or K. Similarly, the inflection temperatures for Na ($T_I \simeq 245$ K, $T_m = 371.0$) and K ($T_I = 225$ K, $T_m = 336.86$) are closer to the respective T_m than that in case of Rb ($T_I \simeq 115$ K, $T_m = 312.47$ K) and Cs ($T_I = 125$ K, $T_m = 301.59$ K).

The inflection in C_p should better be understood by considering all the three contributions C_p^{gas}, C_p^{η} and C_p^{el} separately. As an example, C_p^{gas} and C_p^{η} as a function of T for Na is plotted in Figure 2. C_p^{el} has not been plotted because it is very small in comparison to C_p^{gas} and C_p^{η} and also rises linearly with T. It is evident from Figure 2 that the inflection in C_p as well as the characteristic behaviour of C_p in the undercooled region arise due to structural contribution C_p^{η}. In particular, the inflection in C_p might be a signature of the configurational transformation at T_I and possibly could be viewed as structural freezing. This happens as an outcome of a suitable blending of η and $(\partial\eta/\partial T)$. The latter varies significantly around T_I. In the light of above discussion any

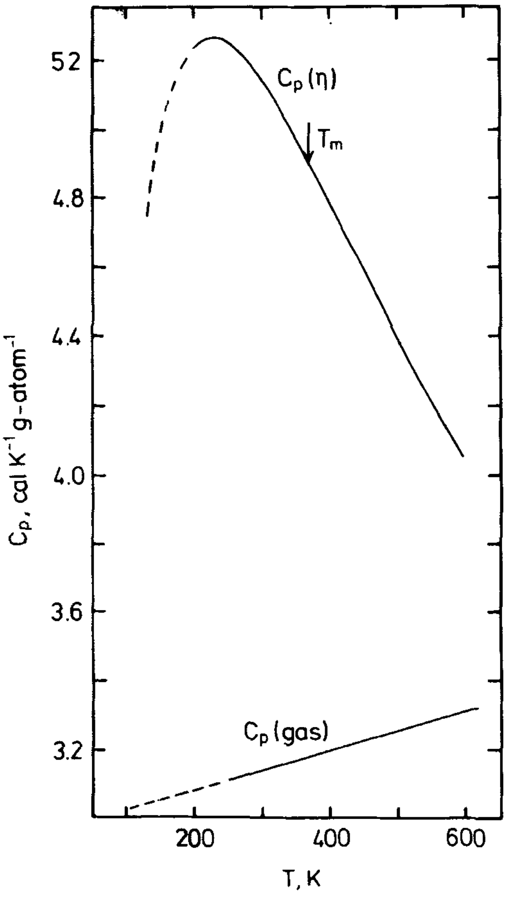

Figure 2 Contributions to specific heat of Na from structural term [C_p^{η}] and the gas term [C_p^{gas}].

extrapolation in the undercooled region beyond T_I has, as such, no physical significance. The loss of entropy due to increasing C_p leads to a negative entropy difference (ΔS) between the undercooled liquid and the stable crystalline state at finite temperature which was first pointed out by Kauzman [23]. This apparent paradox is averted by glass formation. The temperature at which $\Delta S = 0$ is called ideal glass temperature (T_0), i.e.

$$\Delta S(T_0) = \Delta S_m - \int_{T_0}^{T_m} \frac{C_p^l(T) - C_p^S(T)}{T} dT = 0 \tag{21}$$

ΔS_m is the entropy of melting at T_m. The calculated T_0 values for Na, K, Rb and Cs liquid metals using the C_p^l-values given in Figure 1 come out to be lower to T_I ($T_0(\mathrm{Na}) = 126\,\mathrm{K}$, $T_0(\mathrm{K}) = 102.5\,\mathrm{K}$) for Na and K but closer ($T_0(\mathrm{Rb}) = 132.5\,\mathrm{K}$, $T_0(\mathrm{Cs}) = 125\,\mathrm{K}$) for Rb and Cs. From this point of view a calculated C_p^l value below T_0 has also no physical meaning.

The inflection in C_p can also be understood by considering a deviation from the nonlinearity of the energy ($E = E_{\mathrm{el}} + E_{\mathrm{el\text{-}ion}} + E_{\mathrm{ion}}$) function. Among these contributions, E_{el} is negative and its magnitude decreases with decreasing T. Similarly the ionic contribution, E_{ion}, is negative but its magnitude keep increasing with decreasing T in the undercooled region. The electron-ion contribution, $E_{\mathrm{el\text{-}ion}}$, is positive and its magnitude also increases with decreasing temperature. Around T_m, E_{el} and $E_{\mathrm{el\text{-}ion}}$ almost cancel each other and thereby the enthalpy function is dominated by the ionic contribution E_{ion}. But in the undercooled region the repulsive contribution due to $E_{\mathrm{el\text{-}ion}}$ starts playing effective role and contributes significantly to E. So the inflection temperature T_I is an outcome of the interplay of the repulsive energy ($E_{\mathrm{el\text{-}ion}}$) and the attractive energy (E_{ion}). We may emphasize that both E_{ion} and $E_{\mathrm{el\text{-}ion}}$ are structure dependent terms. We intend to persue this point later in the forthcoming publication.

4 STRUCTURE FACTOR

It is of interest to present here the results of the structure factor $S(q)$ in the undercooled region. The values of $S(q)$ computed for Na is plotted in Figure 3. The effect of temperature on $S(q)$ around the principal maximum below the melting point is self evident. As we undergo the T_m, the peaks tend to become sharper and narrower. The peak height increases whereas its width decreases on lowering the temperature. Besides, the temperature effect in the undercooled region is distinctively visible on the long wavelength limit of the direct correlation function, $C\,(q \to 0)$. $S(q)$ is directly related to $C(q)$, i.e.

$$S(q) = \{1 - C(q)\}^{-1} \tag{22}$$

In the long wavelength limit, one simply has

$$S(q \to 0) = \{1 - C(q \to 0)\}^{-1} \tag{23}$$

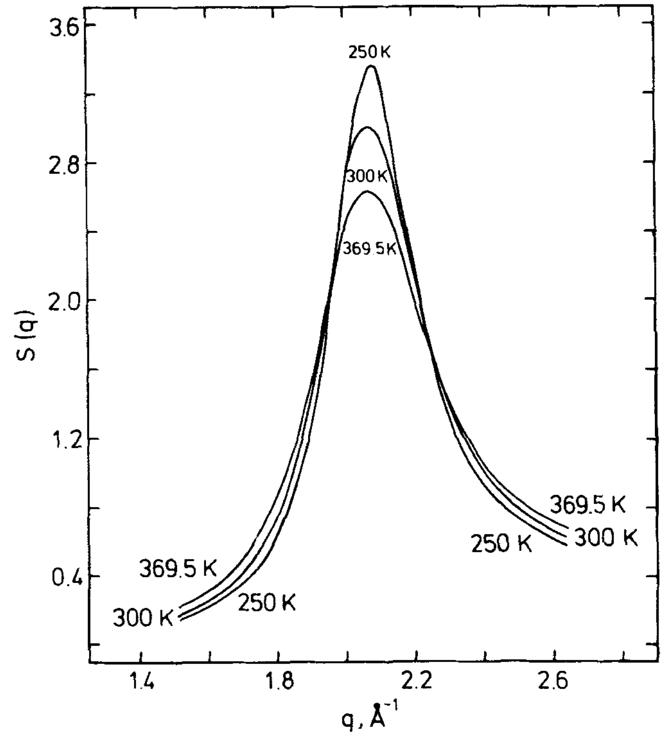

Figure 3 Static structure factor, $S(q)$ of liquid Na in the undercooled region.

The Percus–Yevick (PY) hard-sphere expression for the long wave-length limit of the structure factor is readily expressible in terms of packing fraction η, i.e.

$$S(0) = (1-\eta)^4 (1+2\eta)^{-1} \tag{24}$$

Therefore, $C(q \to 0)$ becomes

$$C(q \to 0) = \eta(2+\eta^2)(\eta-4)(1-\eta)^{-4} \tag{25}$$

Bhatia and March [24] have further noted that for PY solution, $C(q \to 0)$ and $C(r \to 0)$ are simply related to,

$$C(r \to 0) = C(q \to 0) - 1 \tag{26}$$

The values of $S(q \to 0)$ and $C(q \to 0)$ obtained for Na are displayed in Figure 4. It suggests that the gradient of $C(q \to 0)$ becomes quite steep in the undercooled region. The direct correlation function rises sharply and thereby indicating a highly correlated system around T_l.

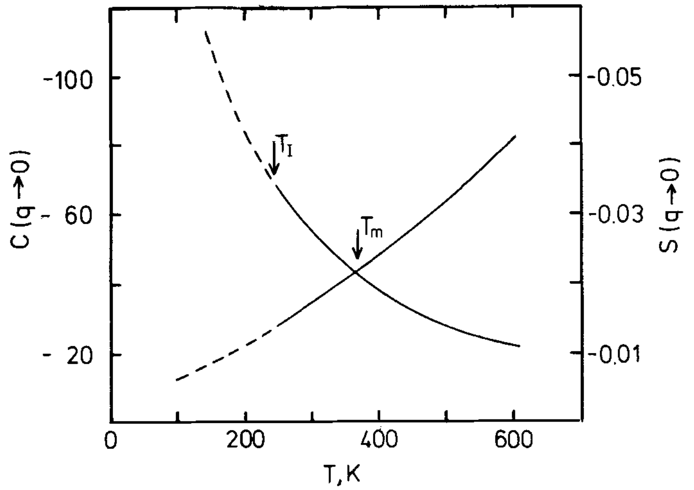

Figure 4 Long wavelength ($q \rightarrow 0$) values of the direct correlation function, $C(q)$ and the structure factor, $S(q)$ in the undercooled ($T < T_m$) and high temperature ($T > T_m$) range of liquid Na.

5 DIFFUSION

It should be useful to investigate the influence of the temperature dependent structural parameter (η) on the diffusion coefficient (D). It has always been a subject of considerable interest to describe the temperature dependence of D for liquid metals both from the experiment [25] and by using simple theoretical models. In fact, it was shown [26] that the diffusion data of many liquid metals, above $T > T_m$, can adequately be described by considering the T-dependence of the packing fraction. In terms of η, D can be expressed as [27]

$$D_\eta = \frac{1}{16}\left(\frac{\pi K_B T}{m}\right)^{1/2}\left(\frac{6\Omega}{\pi\eta^2}\right)^{1/3}\frac{(1-\eta)^3}{(1-0.5\eta)} \tag{27}$$

Though Eq. (27) yields diffusion data of reasonable order of magnitude, it is somewhat larger than the observed data near the melting temperature. For dense hard sphere fluids, the discrepancies could be understood by considering a back scattering effect. For dense packing, one may imagine a cage-like structure of an atom which prevents a free movement after the binary encounter occurs. After making necessary correction, one may write.

$$D = \beta(\eta) D\eta \tag{28}$$

where $\beta(\eta)$ is the correction factor for cage-type structure. The results of computer experiments [28, 29] suggest that $\beta(\eta) = 0.33/\eta$ in the neighbourhood of $\eta = 0.46$. Taking this into account and that of Eq. (27), the temperature dependence of D is calculated. The calculated values of D indicate a T^2 dependence in the undercooled region. It may be recalled here that the spacelab-flight microgravity experiment also exhibit T^2 dependence for D for liquid metals particularly in Sn [30].

As an example, the results of Na computed with Eqs. (27) and (28) are plotted in Figure 5. These are compared with the experimental observations [31] which in a narrow region of temperature, $T \geq T_m$, have been approximated by the expression

$$D = D_0 e^{-Q/RT} \tag{29}$$

where D_0 is a constant and Q is the activation energy. A good attempt has been made by different experimental workers to obtain consistent values for D_0 and Q for liquid Na i.e. $D_0 = 1.1 \times 10^{-3}\,\text{cm}^2\,\text{s}^{-1}$, $Q = 10.2\,\text{kJ}\,\text{mol}^{-1}$, [Meyer and Nachtrieb [32]], $D_0 = 0.92 \times 10^{-3}\,\text{cm}^2\,\text{s}^{-1}$, $Q = 9.79\,\text{kJ}\,\text{mol}^{-1}$ [Ozelton and Swalin [33]] and $D_0 = 0.86 \times 10^{-3}\,\text{cm}^2\,\text{s}^{-1}$, $Q = 9.29\,\text{kJ}\,\text{mol}^{-1}$ [Larsson, Roxberg and Lodding [31]]. The different sets of constants give a closer value for D near the melting point but the discrepancy increases as one goes $T > T_m$. Since the Larson *et al.* [31] values lie in between the other two values, we have plotted them in Figure 5.

The values obtained for Na from the theoretical expression (28) is in very good agreement with the experimental observation near the melting temperature. As expected, the discrepancy increases at temperatures $T > T_m$. It is interesting to observe that the values of D computed at $T > T_m$ with uncorrected Eq. (27) are in better agreement with the observed values than that due to Eq. (28). It seems that the Eq. (28) underestimates the values of D at higher temperature. This happens due to correction factor $\beta(\eta)$. At higher temperature, the correction for cage-like structure which restricts the free movement of atom might not be needed. In this context, we may also recall from Figure 4 that the direct correlation function $C(q \rightarrow 0)$ decays exponentially to a bare

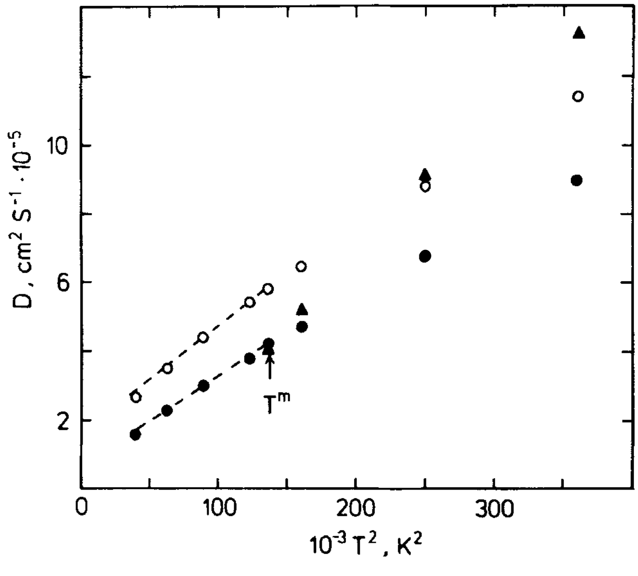

Figure 5 Diffusion coefficient, $D(\text{cm}^2\,\text{s}^{-1})$, for liquid Na as a function of T^2, ○○○ due the equation (27), ●●● due to Eq. (28) and ▲▲▲ refers to experimental empirical Eq. (29).

minimum in the high temperature region. In the light of above discussion, a computer based simulation could be useful for both undercooled and high temperature range of liquid metals.

6 CONCLUSION

A theoretical scheme based on pseudopotential perturbation theory, the thermodynamics of hard sphere systems and the variational method under Gibbs–Bogoliaubov inequality condition is proposed to calculate the specific heat and the diffusion coefficients of liquid metals (Na, K, Rb, Cs) in the undercooled region. The investigations suggest that

(i) C_p in the undercooled ($T < T_m$) region increases with decreasing temperature till it reaches a point of inflection at $T = T_I$. The inflection temperature (T_I) occurs due to structural contribution and has been interpreted as a signature of configurational freezing. The direct correlation function rises sharply and thereby indicating a highly correlated system around T_I.

(ii) D in the undercooled region exhibit T^2 dependence.

References

1. A. T. Dinsdale, "*SGTE Data for Pure Elements*", NPL Report DMA (A) 195 (1989).
2. F. Sommer, to be published (1994).
3. F. Sommer, *Z. Metallkde.*, **73**, 82 (1982).
4. W. L. Johnson, *Prog. Mater. Sci.*, **30**, 81 (1986).
5. L. Battezatti, *Phil. Mag.* B **61**, 81 (1986).
6. A. L. Greer, *J. Less Common Met.*, **145**, 131 (1988).
7. W. Kurz and R. Trivedi, *Acta metall. mater.*, **38**, 1 (1990).
8. W. J. Boettinger and J. H. Perepzeko, Proc. TMS-AIME Northeast Regional Meeting eds. S. K. Das, B. H. Kear, C. M. Kear, C. M. Adam, Metallurgical Society, Ohio, p. 21 (1986).
9. H. Jones, Rapid Solidification of Metals and Alloys, Monograph 8, Institute of Metallurgists, London (1982).
10. W. H. Young, *Rep. Prog. Phys.*, **55**, 1769 (1992).
11. H. Jones, *J. Chem. Phys.*, **55**, 2640 (1971).
12. W. A. Harrison, Pseudopotential in the Theory Metal (New York: Benjamin) (1966).
13. V. Heine, and I. V. Abarenkov, *Phil. Mag.*, **9**, 451 (1964).
14. M. L. Cohen and V. Heine, *Solid State Physics*, **14**, 3137 (1970).
15. Ese and J. A. Reissland, *J. Phys. F. Metal Phys.*, **3**, 2066 (1973).
16. P. Noziers and D. Pines, *Phys. Rev.* **111**, 442 (1958).
17. J. Hafner and P. Schmuck, *Phys. Rev.*, **39**, 4138 (1974).
18. N. W. Ashcroft and J. Lekner, *Phys. Rev.*, **145**, 83 (1966).
19. E. A. Brandes, *Smithells Metals Reference Book* (ed.) Butterworth, London (1983).
20. R. N. Singh and V. N. Singh, *Phys. Chem. Liq.*, **22**, 235 (1991).
21. T. Shen and J. T. Wang, *J. Non Crystalline Solids*, **117**, **118**, 559 (1990).
22. J. H. Perepezko and J. S. Paik, *J. Non Crystalline Solids*, **61**, **62**, 113 (1984).
23. W. Kauzmann, *Chem. Rev.*, **43**, 219 (1948).
24. A. B. Bhatia and N. H. March, *J. Chem. Phys.*, **80**, 2076 (1984).
25. N. H. Nachtrieb, in "The Properties of Liquid Metals (S. Takeuchi ed.) Taylor S. Francis, London, p. 521 (1973).
26. P. Protopapas, H. C. Anderson and N. A. D. Parter, *J. Chem. Phys.*, **59**, 15 (1973).
27. T. E. Faber, "*An Introduction to the Theory of Liquid Metals*", Cambridge University Press, London (1972).
28. B. J. Alder and T. E. Wainwright, *Phys. Rev. Lett.*, **18**, 988 (1967).

29. B. J. Alder, D. M. Gass and T. E. Wainright, *J. Chem. Phys.*, **53**, 3813 (1970).
30. G. Frohberg, K. H. Kraatz and H. Wever, in "*Scientific results of the German Mission D1*", Proc. of the Norderney Symp. WPF/DLR, Köln, p. 144 (1987).
31. S. J. Larson, C. Rosbergh and A. Lodding, *Phys. Chem. Liquid*, **3**, 137 (1972).
32. R. E. Meyer and N. H. Nachtrieb, *J. Chem. Phys.*, **23**, 1851 (1955).
33. M. W. Ozelton and R. A. Swalin, *Phil. Mag.*, **18**, 441 (1968).